Supporting Information

Fe,N Co-doped Mesoporous Carbon Nanosheets for Oxygen Reduction

Peng Du [a,b,c,†], Xufen Xiao [a,b,c,†], Feixiang Ma [a,b,c,d], Hao Wang [a,b,c,d], Junda Shen [a,c,d], Fucong Lyu [a,c,d], Yingxian Chen [a,c,d], Jian Lu [b,c,d,e,], Yangyang Li [a,b,c,d,*]*

[a] *Center of Super-Diamond and Advanced Films (COSDAF), City University of Hong Kong, Kowloon, 000000, Hong Kong, P.R. China*

[b] *Department of Material Science and Engineering, City University of Hong Kong, Kowloon, 000000, Hong Kong, P.R. China*

[c] *Hong Kong Branch of National Precious Metals Material Engineering Research Centre (NPMM), City University of Hong Kong, Kowloon, 000000, Hong Kong, P.R. China*

[d] *Department of Mechanical Engineering, City University of Hong Kong, Greater Bay Joint Division, Shenyang National Laboratory for Materials Science, Tat Chee Avenue, Kowloon, 000000, Hong Kong, P.R. China*

[e] *Center for Advanced Structural Materials, City University of Hong Kong Shenzhen Research Institute, Greater Bay Joint Division, Shenyang National Laboratory for Materials Science, 8 Yuexing 1st Road, Shenzhen Hi-Tech Industrial Park, Nanshan District, Shenzhen, 518000, P.R. China*

*Corresponding Author: *E-mail: jianlu@cityu.edu.hk (Jian Lu). *E-mail: yangli@cityu.edu.hk (Yangyang Li).*

Table of Contents

Section 1. Abbreviations and Characters

Abbreviations

SEM ----- Scanning Electron Microscopy

AFM ----- Atomic Force Microscopy

HRTEM ----- High-Resolution Transmission Electron Microscopy

HAADF-STEM - High Angle Annular Dark Field Scanning Transmission Electron Microscopy

EDXS ----- Energy Dispersive X-ray Spectroscopy

XRD ----- X-ray diffraction

BET ----- Brunauer-Emmett-Teller

XPS ----- X-ray photoelectron spectroscopy

SCE ----- saturated calomel electrode

RHE ----- Reversible Hydrogen Electrode

RDE ----- Rotating Disk Electrode

RRDE ----- Rotating Ring-Disk Electrode

GC ----- Glassy Carbon

Characters

J ----- Current Density

J_K ----- Kinetic Current Density

J_L ----- Limiting Current Density

ω ----- Angular Velocity,

n ----- Total Electron Transfer Number

F ----- Faraday Constant (96485 C mol^{-1})

C_0 ----- Bulk Concentration of O_2 (1.2×10^{-6} $mol \cdot cm^{-3}$ in 0.1 M KOH)

D_0 ----- Diffusion Coefficient of O_2 (1.9×10^{-5} $cm^2 \cdot s^{-1}$ in 0.1 M KOH)

V ----- Kinematic Viscosity of the Electrolyte (0.01 $cm^2 \cdot s^{-1}$ in 0.1 M KOH)

I_D ----- Disk Current

I_R ----- Ring Current

N ----- Ring Collection Coefficient ($N = 0.37$)

Section 4. Supplementary Figures

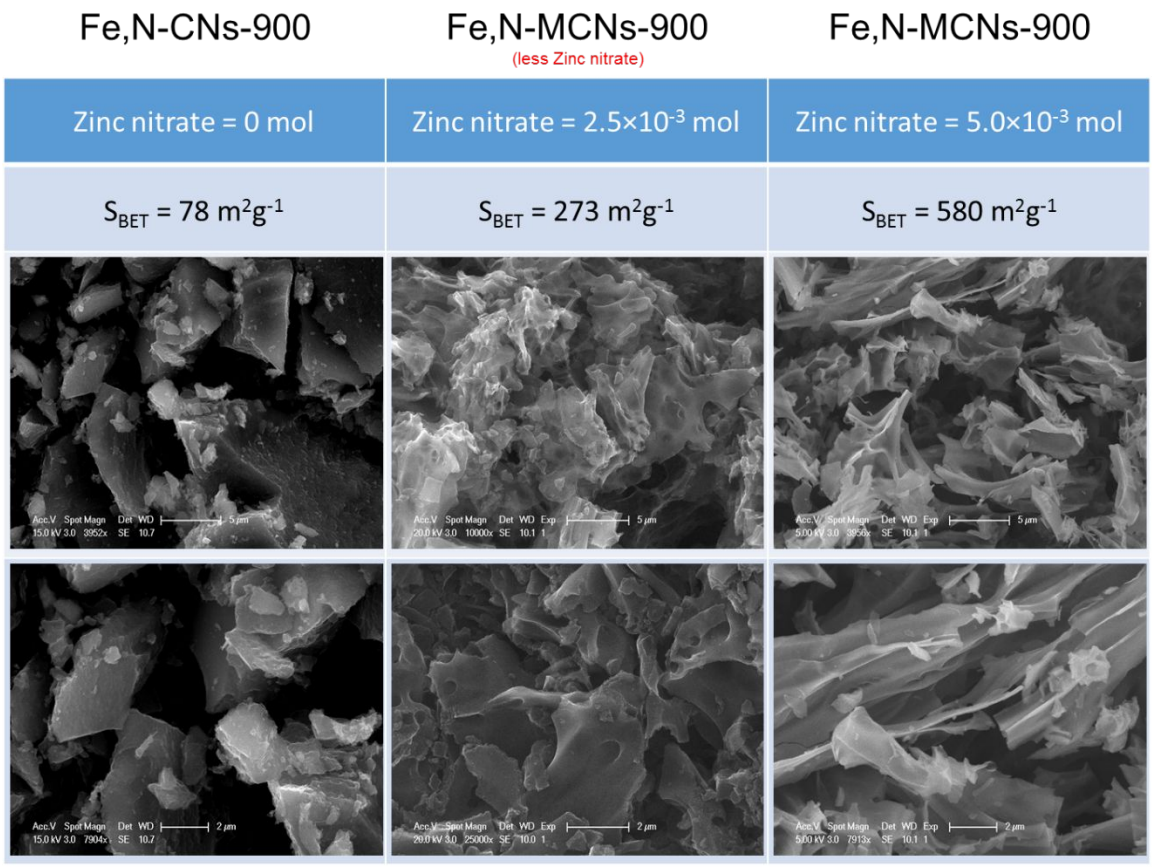

Figure S1. Comparison of morphology and specific surface area of the samples with different amounts of zinc nitrate added.

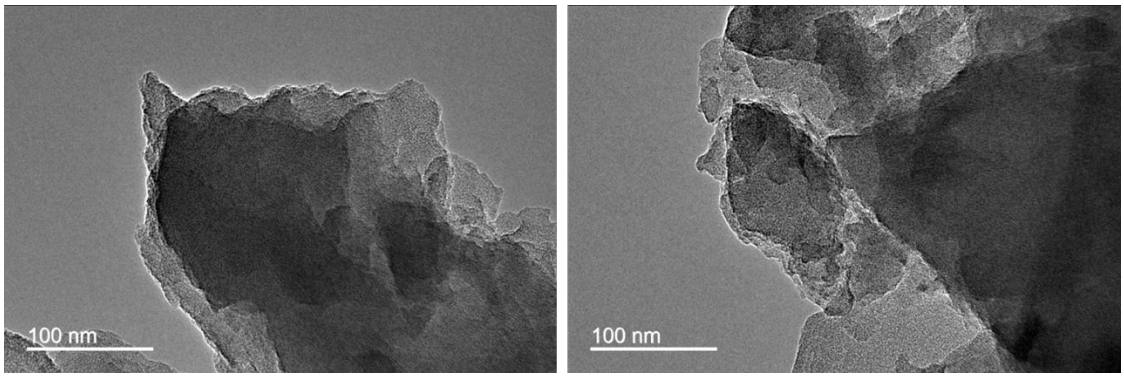

Figure S2. TEM images of Fe,N-CNs-900.

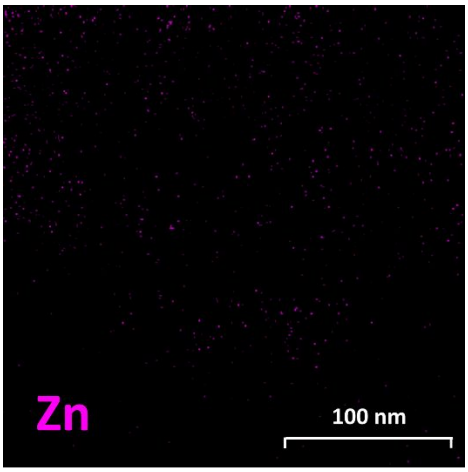

Figure S3. EDX mapping for Zn element of Fe,N-MCNs-500

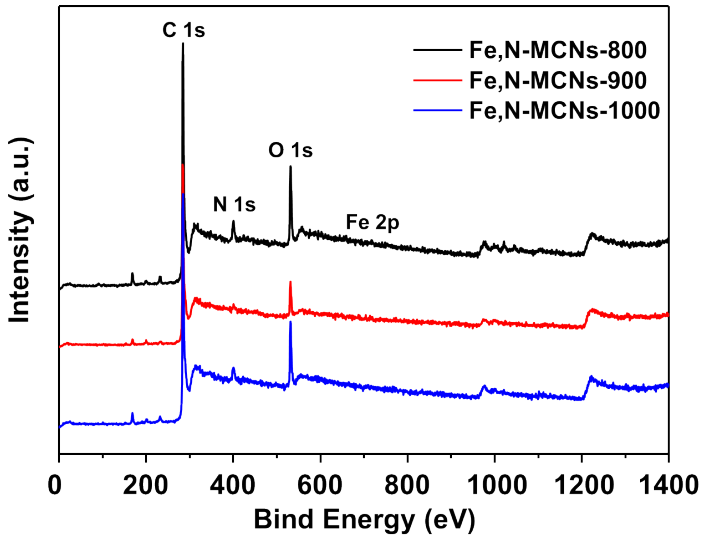

Figure S4. XPS survey spectra of Fe,N-MCNs-800, -900 and -1000.

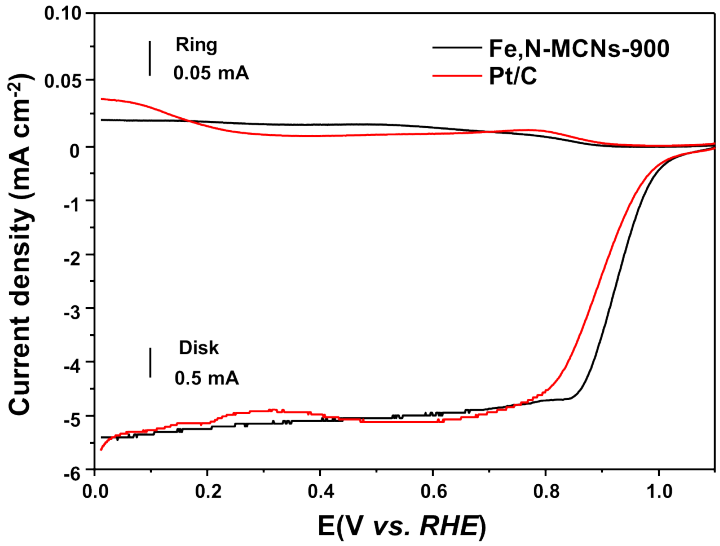

Figure S5. LSV curves of Fe,N-MCNs-900 and commercial 20% Pt/C catalyst measured on RRDE at 1600 rpm in O_2-saturated 0.1 M KOH. Ring potential: 1.5 V *vs. RHE*.

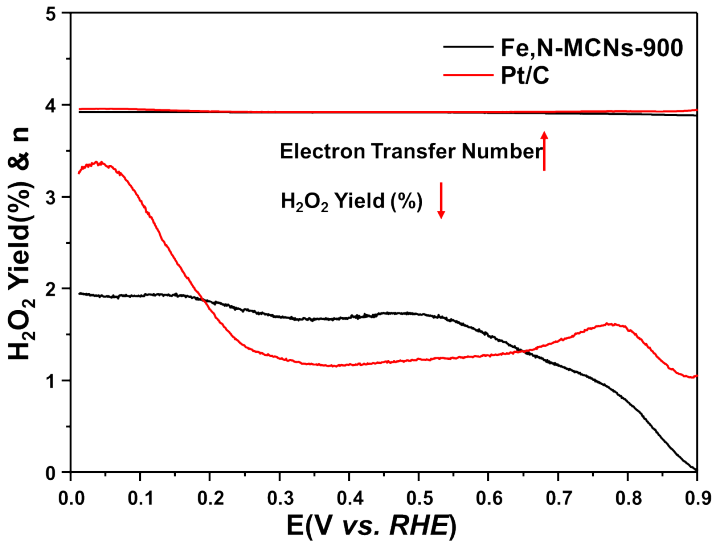

Figure S6. The dependence of electron transfer number *n* on the potential and the H_2O_2 generation for Fe,N-MCNs-900 catalyst calculated from the corresponding RRDE data.

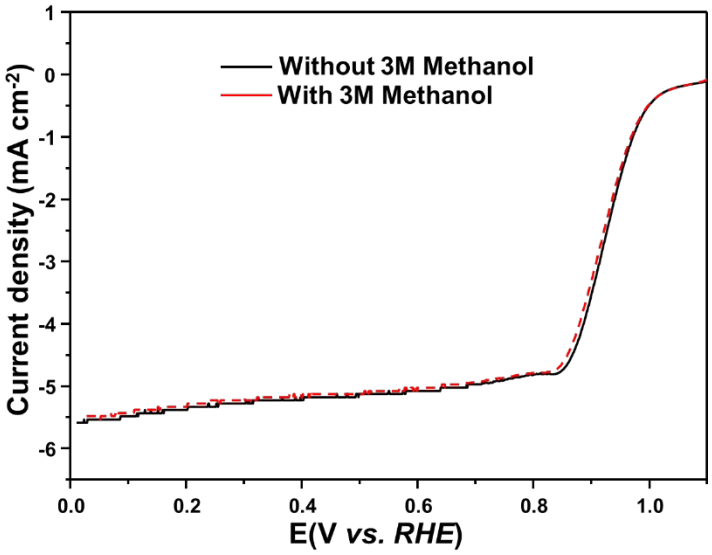

Figure S7. LSVs of Fe,N-MCNs-900 catalyst in O_2-saturated 0.1M KOH without and with 3M CH_3OH.

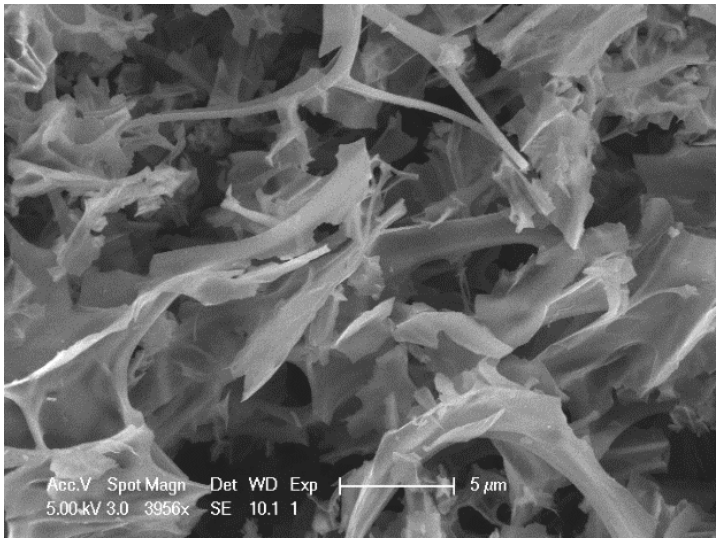

Figure S8. SEM image of Fe,N-MCNs-900 after the catalytic stability test.

Section 2. Supplementary Tables

Table S1. The elements contents for different catalysts. **(Unit: wt.%)**

Samples	N 1s	Fe	Zn
Fe,N-MCNs-800	7.48	0.42	0.46
Fe,N-MCNs-900	6.50	0.53	0.31
Fe,N-MCNs-1000	2.37	0.54	0.06
Fe,N-CNs-900	3.48	0.34	/

Table S2. The contents of pyridinic-N and Fe-N_x species for different catalysts. **(Unit: wt.%)**

Samples	N 1s	pyridinic-N	Fe-N_x
Fe,N-MCNs-800	7.48	1.56	0.76
Fe,N-MCNs-900	6.50	1.40	1.05
Fe,N-MCNs-1000	4.32	0.53	0.92
Fe,N-CNs-900	5.47	0.55	0.82

Table S3. The proportion of active species (pyridinic-N and Fe-N_x) for the different catalysts.

Samples	pyridinic-N	Fe-N_x	Total
Fe,N-MCNs-800	20.91%	10.11%	31.02%
Fe,N-MCNs-900	21.55%	16.19%	37.74%
Fe,N-MCNs-1000	12.24%	21.25%	33.49%
Fe,N-CNs-900	10%	15%	25%

Table S4. Comparison of ORR catalytic performances in alkaline solution between Fe,N-MCNs series catalysts and other previously reported catalysts.

Catalyst	E_{onset} (V) [#]	$E_{1/2}$ (V) [^]	Electrolyte	Reference
Fe,N-MCNs-800	0.98	0.89	0.1 M KOH	This work
Fe,N-MCNs-900	**0.99**	**0.92**	**0.1 M KOH**	**This work**
Fe,N-MCNs-1000	0.99	0.90	0.1 M KOH	This work
CoFe@C	0.98	0.89	0.1 M KOH	*1*
Co_3O_4/rmGO	0.88	0.83	0.1 M KOH	*2*
Fe-N/C-800	0.92	0.81	0.1 M KOH	*3*
Co_9S_8@CNS900	0.91	0.79	0.1 M KOH	*4*
Co@Co_3O_4@CCM	0.93	0.81	0.1 M KOH	*5*
Fe_3C@N-CNT	-	0.85	0.1 M KOH	*6*
CoZn-NC-700	-	0.84	0.1 M KOH	*7*
NPMC-1000	0.94	0.85	0.1 M KOH	*8*
PMF-800	-	0.86	0.1 M KOH	*9*
ZnN_x/BP	~0.99	0.84	0.1 M KOH	*10*

[#] E_{onset} is the onset potential of ORR. All the potentials are *versus* the RHE.

[^] $E_{1/2}$ is the half-wave potential of ORR. All the potentials are versus the RHE.

Section 3. References

(1) Zhao, R.; Liang, Z.; Gao, S.; Yang, C.; Zhu, B.; Zhao, J.; Qu, C.; Zou, R.; Xu, Q. Puffing up Energetic Metal-Organic Frameworks to Large Carbon Networks with Hierarchical Porosity and Atomically Dispersed Metal Sites. *Angew. Chem.* 2019, 131, 1997-2001.

(2) Liang, Y.; Li, Y.; Wang, H.; Zhou, J.; Wang, J.; Regier, T.; Dai, H. Co_3O_4 Nanocrystals on Graphene as a Synergistic Catalyst for Oxygen Reduction Reaction. *Nat. Mater.* 2011, 10, 780-786.

(3) Lin, L.; Zhu, Q.; Xu, A.W. Noble-Metal-Free Fe-N/C Catalyst for Highly Efficient Oxygen Reduction Reaction under Both Alkaline and Acidic Conditions. *J. Am. Chem. Soc.* 2014, 136, 11027-11033.

(4) Zhu, Q. L.; Xia, W.; Akita, T.; Zou, R.; Xu, Q. Metal-Organic Framework-Derived Honeycomb-Like Open Porous Nanostructures as Precious-Metal-Free Catalysts for Highly Efficient Oxygen Electroreduction. *Adv. Mater.* 2016, 28, 6391-6398.

(5) Xia, W.; Zou, R.; An, L.; Xia, D.; Guo, S. A Metal-Organic Framework Route to In Situ Encapsulation of Co@Co_3O_4@C Core@Bishell Nanoparticles into a Highly Ordered Porous Carbon Matrix for Oxygen Reduction. *Energy Environ. Sci.* 2015, 8, 568-576.

(6) Guan, B. Y.; Yu, L.; Lou, X. W. D. A Dual-Metal-Organic-Framework Derived Electrocatalyst for Oxygen Reduction. *Energy Environ. Sci.* 2016, 9, 3092-3096.

(7) Chen, B.; He, X.; Yin, F.; Wang, H.; Liu, D. J.; Shi, R.; Chen, J.; Yin, H. MO-Co@N-Doped Carbon (M= Zn or Co): Vital Roles of Inactive Zn and Highly Efficient Activity toward Oxygen Reduction/Evolution Reactions for Rechargeable Zn-Air Battery. *Adv. Funct. Mater.* 2017, 27, 1700795.

(8) Zhang, J.; Zhao, Z.; Xia, Z.; Dai, L. A Metal-Free Bifunctional Electrocatalyst for Oxygen Reduction and Oxygen Evolution Reactions. *Nat. Nanotechnol.* 2015, 10, 444.

(9) Yang, W.; Liu, X.; Yue, X.; Jia, J.; Guo, S. Bamboo-Like Carbon Nanotube/Fe_3C Nanoparticle Hybrids and Their Highly Efficient Catalysis for Oxygen Reduction. *J. Am. Chem. Soc.* 2015, 137, 1436-1439.

(10) Song, P.; Luo, M.; Liu, X.; Xing, W.; Xu, W.; Jiang, Z.; Gu, L. Zn Single Atom Catalyst for Highly Efficient Oxygen Reduction Reaction. *Adv. Funct. Mater.* 2017, 27, 1700802.